Theoretical study on the cylinder-shaped N_{78} cage

Hongwei Zhou [a], Ning-Bew Wong [b,**], Anmin Tian [a,*]

[a] Faculty of Chemistry, Sichuan University, Chengdu 610064, People's Republic of China
[b] Department of Biology and Chemistry, City University of Hong Kong,
Kowloon, Hong Kong, People's Republic of China

Abstract

Recent theoretical studies have suggested that the stabilizing factors for large nitrogen cages tend to favor more five-membered rings, more three-membered rings and cylindrical structure with large numbers of layers. Further studies of relative stability of the all-nitrogen molecule have prompted to figure out what brings about the stabilizing factors. Herein, the cylinder-shaped molecule of N_{78} (D_{3h}) has been studied in detail. The geometry and energies are examined at B3LYP/cc-pVDZ and single point energy calculations at MP2/cc-pVDZ are carried out for the purposes of determining relative thermodynamic stability. NBO analysis and AIM analysis are applied to investigate the bonding properties of the cage molecule. The major result of this study is the identification of intra-molecular interactions, whether it is at B3LYP/cc-pVDZ or at MP2/cc-pVDZ, as the dominant stabilizing factor for the large all-nitrogen cage. The length of the cylinder-shaped molecule is about 2.5 nm. N_{78} (D_{3h}) might be one novel nanomaterial which is environment-friendly and as a beeline nanotube or a beeline ''nano-bar'', it is expected to impact a wide range of applications.
© 2006 Elsevier Inc. All rights reserved.

Keywords: Cylinder-shaped N_{78} cage; Stabilizing factor; Intra-molecular interaction

1. Introduction

Molecules consisting entirely or predominantly of nitrogen are the focus of much research for their potential as high energy density materials (HEDM) [1–24], due to the dissociation of all-nitrogen molecule into N_2 molecules with the release of a large amount of energy, which can be used as propellants and explosives [1]. However, in order to be considered a viable candidate for HEDM, all-nitrogen molecules need to possess a resistance to decomposition to some extent. The difficulty lies in estimating all-nitrogen molecules that are metastable enough to serve as stable fuels. So, the relative stabilities of all-nitrogen molecules become the focus of recent experimental and theoretical research. The stabilities of an even number of atoms N_{2n} molecules have been studied in a computational survey of various structural forms with up to 60 atoms. Cyclic, acyclic, and cage isomers have been studied to examine the bonding properties and energy properties over a wide range of

molecules, such as N_4 [1,2], N_6 [1–3], N_8 [1–3,5–10] N_{10} [1,10–15], N_{12} [1,10,14,17,18], N_{14} [10,19,20], N_{16} [10], N_{18} [21], N_{20} [10,12,22], N_{24} [10,23,24], N_{30} [12,23], N_{32} [24], N_{36} [23], N_{42} [24], N_{48} [24], N_{54} [24], N_{56} [24] and N_{60} [11,22,24,25]. The computational studies of cage isomers of N_{12} [17], N_{24} [23], N_{30} [23] and N_{36} [23] examined specific structural features that lead to the most stable molecules among the three-coordinate nitrogen cages. Those results showed that molecules with the most five-membered rings (referred to as pentagons) in the nitrogen network tend to be the most stable, with a secondary stabilizing effect due to three-membered rings (referred to as triangles) in the cage structure. Meanwhile, Strout [23] have pointed out that the cylinder-shaped nitrogen cages are more stable than the other shape. Our recent theoretical predictions on cage stability for N_{2n} (N_6 (D_{3h}), N_8 (O_h), N_{10} (D_{5h}), N_{12} (D_{6h}), N_{12} (D_{3d}), N_{16} (D_{4d}), N_{18} (D_{3h}), N_{20} (I_h), N_{24} (D_{3d}), N_{24} (D_{4h}), N_{24} (D_{6d}), N_{30} (D_{3h}), N_{30} (D_{5h}), N_{32} (D_{4d}), N_{36} (D_{3d}), N_{40} (D_{4h}), N_{42} (D_{3h}), N_{48} (D_{4d}), N_{48} (D_{3d}), N_{54} (D_{3h}), N_{56} (D_{4h}) and N_{60} (D_{3d})) [22] indicate that the most thermodynamically stable isomer has three-fold symmetry (D_{3h} or D_{3d} symmetry point group). Such molecules have a triangle-pentagon bonding group on each end with a band of hexagons around the midsection. However, the existence of this

---

* Corresponding author. Tel.: +86 28 8541 2800; fax: +86 28 8541 2800.
** Corresponding author.
  E-mail address: suqcp@mail.sc.cninfo.net (A. Tian).
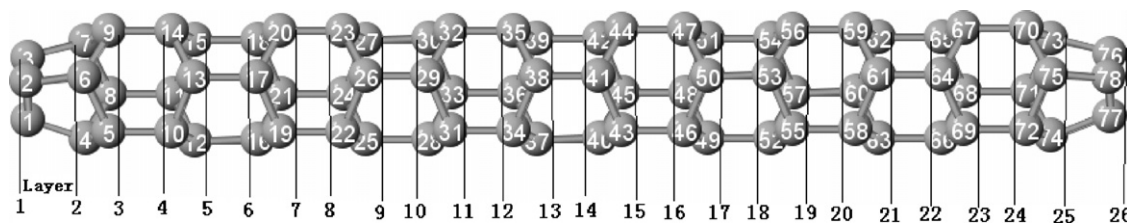
Fig. 1. The structure and the layers of the N_{78} (D_{3h}) cage.

symmetric isomer depends on the number of nitrogen atoms being a multiple of three or on the number of layers. Besides these factors, are there any other factors that render the cylinder-shaped nitrogen cage to be stable? Such reports have not been seen. Cage molecule N_{78} (D_{3h}) with these features has never studied before as well.

2. Computational methods

For the convenience of constructing the cage N_{78} (D_{3h}), the concept of "layer" is introduced in this work. The term "layer" can be defined as: (i) all atoms belonging to the same layer are coplanar, (ii) all layers in one molecule are parallel to each other, and (iii) all planes in one molecule are perpendicular to its C_3 principal axis. According to this definition, the layers of the molecule and the atoms in each layer of the molecule are shown in Fig. 1.

The molecule N_{78} (D_{3h}) can be constructed as the same manner as ref. 24: At first, N_6 (D_{3h}) cage molecule is chosen as the mother molecule. N_6 (D_{3h}) has two parallel layers called top layer and bottom layer, respectively. Then, one W-shape (chair-form) six-membered ring (referred to as hexagon) is inserted

into the mother molecule. The atoms in the hexagon link to the atoms in the top layer and link to the atoms in the bottom layer of the mother molecule in an alternating manner. Thus, the cage molecule N_{12} (D_{3d}) is formed. In the molecule N_{12} (D_{3d}), the three atoms in the hexagon linking to the top layer atoms of the mother molecule form one layer, and the remaining three atoms in the hexagon linking to the bottom layer atoms form another one. There are four layers in molecule N_{12} (D_{3d}). Analogously, the cage molecule N_{18} (D_{3h}) can be considered as two hexagons with W-shape being inserted into the mother molecule. The molecules N_{24} (D_{3d}), N_{30} (D_{3h}), N_{36} (D_{3d}), N_{42} (D_{3h}), N_{48} (D_{3d}), N_{54} (D_{3h}), N_{60} (D_{3d}), N_{66} (D_{3h}), N_{72} (D_{3d}) and N_{78} (D_{3h}) can be formed in the same way. So, cage molecule N_{78} (D_{3h}) can be regarded as the derivative of 12 hexagons being inserted into the mother molecule. Two new layers are added when one W-shaped hexagon is inserted into the mother molecule. Thus, the molecule N_{78} (D_{3h}) contains 26 layers. Each layer contains three nitrogen atoms. The atoms in the same layer are not conjoin and only join to the atoms of the previous layer and the next layer except layers 1 and 26.

We have carried out theoretical studies of the N_{78} (D_{3h}) cage using Gaussian 98 A.11 packages [26]. Density functional

Table 1
The covalent bonds or intra-molecular interactions in every set of the N_{78} (D_{3d}) cage at B3LYP/cc-pVDZ

Type	Num[a]	Bond
35B	6	N_1–N_2, N_1–N_3, N_2–N_3, N_{76}–N_{77}, N_{76}–N_{78}, N_{77}–N_{78}
55B	6	N_1–N_4, N_2–N_6, N_3–N_7, N_{73}–N_{76}, N_{74}–N_{77}, N_{75}–N_{78}
56B	12	N_4–N_5, N_4–N_8, N_5–N_6, N_6–N_9, N_7–N_8, N_7–N_9, N_{70}–N_{73}, N_{70}–N_{75}, N_{71}–N_{73}, N_{71}–N_{74}, N_{72}–N_{74}, N_{72}–N_{75}
66B1	33	N_5–N_{10}, N_8–N_{11}, N_9–N_{14}, N_{12}–N_{16}, N_{13}–N_{17}, N_{15}–N_{18}, N_{19}–N_{22}, N_{20}–N_{23}, N_{21}–N_{24}, N_{25}–N_{28}, N_{26}–N_{29}, N_{27}–N_{30}, N_{31}–N_{34}, N_{32}–N_{35}, N_{33}–N_{36}, N_{37}–N_{40}, N_{38}–N_{41}, N_{39}–N_{42}, N_{43}–N_{46}, N_{44}–N_{47}, N_{45}–N_{48}, N_{49}–N_{52}, N_{50}–N_{53}, N_{51}–N_{54}, N_{55}–N_{58}, N_{56}–N_{59}, N_{57}–N_{60}, N_{61}–N_{64}, N_{62}–N_{65}, N_{63}–N_{66}, N_{67}–N_{70}, N_{68}–N_{71}, N_{69}–N_{72}
66B2	60	N_{10}–N_{12}, N_{10}–N_{13}, N_{11}–N_{12}, N_{11}–N_{15}, N_{13}–N_{14}, N_{14}–N_{15}, N_{16}–N_{19}, N_{16}–N_{21}, N_{17}–N_{19}, N_{17}–N_{20}, N_{18}–N_{20}, N_{18}–N_{21}, N_{22}–N_{25}, N_{22}–N_{26}, N_{23}–N_{26}, N_{23}–N_{27}, N_{24}–N_{25}, N_{24}–N_{27}, N_{28}–N_{31}, N_{28}–N_{33}, N_{29}–N_{31}, N_{29}–N_{32}, N_{30}–N_{32}, N_{30}–N_{33}, N_{34}–N_{37}, N_{34}–N_{38}, N_{35}–N_{38}, N_{35}–N_{39}, N_{36}–N_{37}, N_{36}–N_{39}, N_{40}–N_{43}, N_{40}–N_{45}, N_{41}–N_{43}, N_{41}–N_{44}, N_{42}–N_{44}, N_{42}–N_{45}, N_{46}–N_{49}, N_{46}–N_{50}, N_{47}–N_{50}, N_{47}–N_{51}, N_{48}–N_{49}, N_{48}–N_{51}, N_{52}–N_{55}, N_{52}–N_{57}, N_{53}–N_{55}, N_{53}–N_{56}, N_{54}–N_{56}, N_{54}–N_{57}, N_{58}–N_{61}, N_{58}–N_{63}, N_{59}–N_{61}, N_{59}–N_{62}, N_{60}–N_{62}, N_{60}–N_{63}, N_{64}–N_{67}, N_{64}–N_{69}, N_{65}–N_{67}, N_{65}–N_{68}, N_{66}–N_{68}, N_{68}–N_{69}
V1[b]	6	N_4–N_{12}, N_6–N_{13}, N_7–N_{15}, N_{64}–N_{75}, N_{65}–N_{73}, N_{66}–N_{74}
V2	27	N_{10}–N_{19}, N_{14}–N_{20}, N_{11}–N_{21}, N_{16}–N_{25}, N_{17}–N_{26}, N_{18}–N_{27}, N_{22}–N_{31}, N_{23}–N_{32}, N_{24}–N_{33}, N_{28}–N_{37}, N_{29}–N_{38}, N_{30}–N_{39}, N_{34}–N_{43}, N_{35}–N_{44}, N_{36}–N_{45}, N_{40}–N_{49}, N_{41}–N_{50}, N_{42}–N_{51}, N_{46}–N_{55}, N_{47}–N_{56}, N_{48}–N_{57}, N_{52}–N_{63}, N_{53}–N_{61}, N_{54}–N_{62}
LP1	6	N_1, N_2, N_3, N_{76}, N_{77}, N_{78}
LP2	6	N_4, N_6, N_7, N_{73}, N_{74}, N_{74}
LP3	6	N_5, N_8, N_9, N_{70}, N_{71}, N_{72}
LP4	60	N_{10}–N_{69}

[a] The number of bonds or intra-molecular interactions or lone pairs in every set of the molecule.
[b] The intra-molecular interactions V1 vanish at MP2/cc-pVDZ.

Table 2
Covalent bond length and orbital energies (a.u.) of the N_{78} (D_{3h}) cage at B3LYP/cc-pVDZ

	Length (Å)	Occup[a]	OE	TSEE[b]
35B (N_1–N_2)	1.529	1.954	−0.70758	31.8
55B (N_1–N_4)	1.428	1.975	−0.89766	−1.1
56B (N_4–N_5)	1.483	1.976	−0.84644	1.6
66B1 (N_5–N_{10})	1.483	1.970	−0.86773	−6.3
66B2 (N_{10}–N_{12})	1.459	1.984	−0.88356	−0.9
LP1 (N_1)		1.952	−0.58255	−20.4
LP2 (N_4)		1.894	−0.50018	0.4
LP3 (N_5)		1.924	−0.49062	−3.2
LP4 (N_{10})		1.913	−0.47696	3.0

[a] Electron occupancy of orbital.
[b] Occupied NLMO contributions dE(i) (kcal/mol) to total steric exchange energy.

theory (DFT) has been applied to optimize the structures of N_{78} (D_{3h}) at basis set cc-pVDZ. The single-point energies of the molecule have been carried out at MP2/cc-pVDZ to obtain the wave functions. The optimized structure of N_{78} (D_{3h}) at B3LYP/cc-pVDZ is shown in Fig. 1.

The bond in the cage molecule can be considered as the shared edge of two vicinal rings. So, the vicinal rings on two sides of the shared edge directly affect the bonding properties. If the numbers of atoms in the rings on two sides of the bond are m ($m = 3$–6) and n ($n = 3$–6), respectively, then the bond type is defined as **mn** ($m \leq n$) bond (*ab.* **mn**B) in this work. There are

five sets of bond in the cage molecule N_{72} (D_{3d}), **35B**, **55B**, **56B**, **66B** (**66B1**, **66B2**); two sets of intra-molecular interactions, denoted by **V1** and **V2**, respectively; four sets of lone pair, denoted by **LP1**, **LP2**, **LP3** and **LP4**, respectively. The bonds or the intra-molecular interactions or the lone pairs in every set are listed in Table 1. It is noted that the bonding properties are equivalent in the same set. The geometrical parameters are listed in Table 2.

The topological properties of bonds in molecules have significant influence on the thermodynamic stability of the molecule. So, natural bond orbital (NBO) analysis [27] and atoms in molecule (AIM) analysis [28] are carried out to study the bonding properties. The orbital energies, occupancies, and the steric exchange energies from NBO analysis are listed in Table 2.

AIM analysis has been performed to obtain the topological properties of the electron density, such as the Laplacian of ρ ($\nabla^2\rho$), the bond critical points (BCPs), the ring critical points and the cage critical points, and the bond paths, the ring paths, the cage paths, and the distances between the BCPs and the atoms. The $\nabla^2\rho$ identifies whether the charge of the region is locally depleted ($\nabla^2\rho > 0$) or concentrated ($\nabla^2\rho < 0$). The former is typically associated with interactions between closed-shell systems (ionic bonds, hydrogen bonds, and van der Waals' molecules), whereas the latter characterizes covalent bonds, where the electron density concentrates in the internuclear region. Obviously, the latter is required for
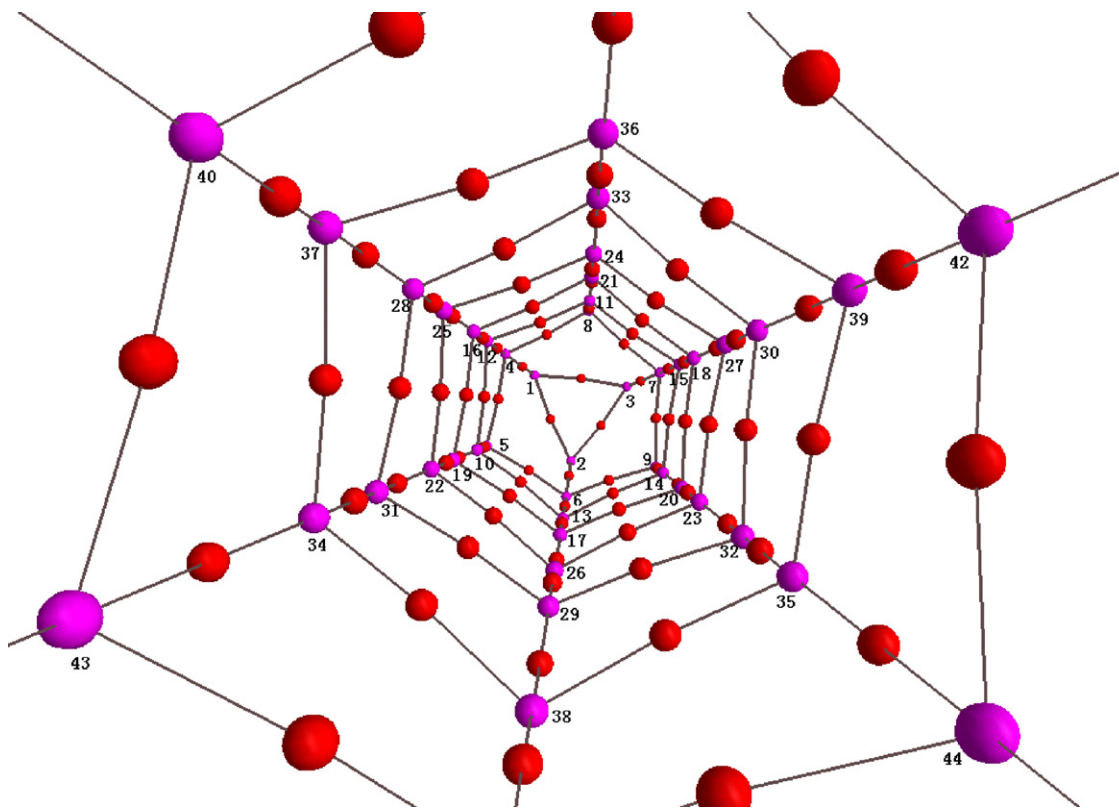

Fig. 2. Parts of the BCPs (the unmarked balls) and the bond paths (lines) of the N_{78} (D_{3h}) cage at B3LYP/cc-pVDZ viewed from the *X*-axis direction. Atoms are marked by digits. There are three intra-molecular interactions between layers 2 and 5 and three intra-molecular interactions between layers 22 and 25 at B3LYP/cc-pVDZ. These six intra-molecular interactions do not exist at MP2/cc-pVDZ.
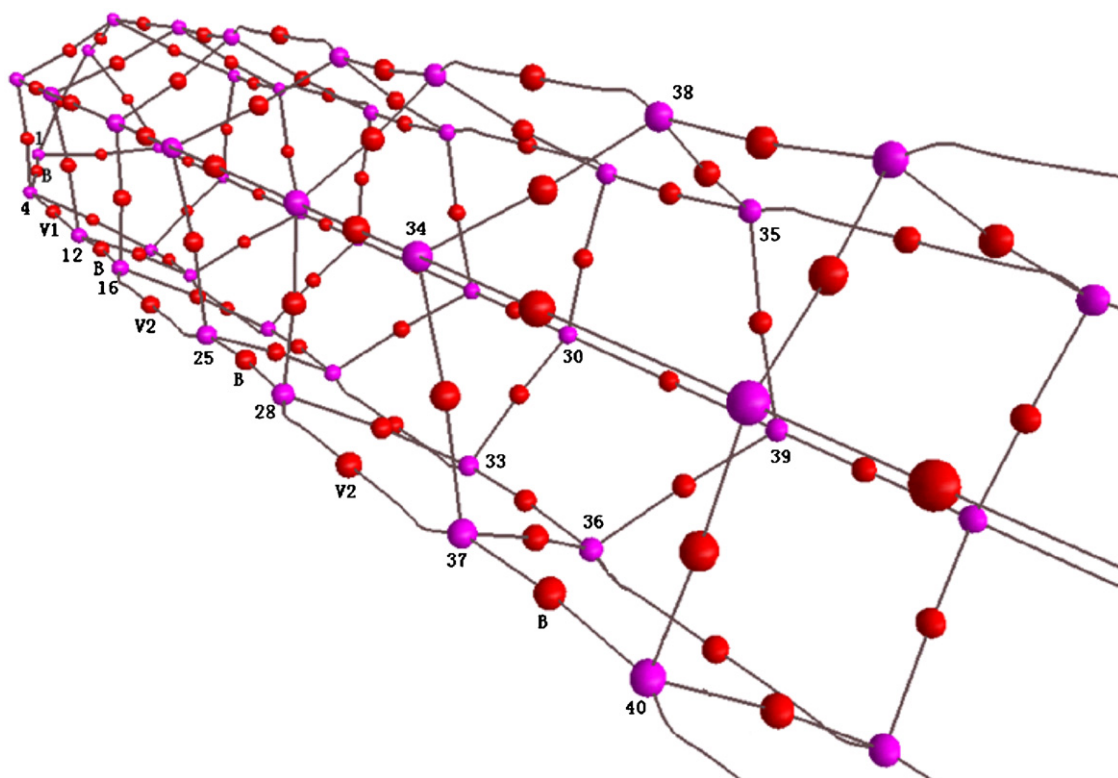
Fig. 3. Parts of the BCPs and the bond paths (lines) of the N_{78} (D_{3h}) cage at B3LYP/cc-pVDZ viewed from the flank of X-axis. Atoms are marked by digits. B: represents the BCP of covalent bond, V: represents the intra-molecular interactions.

covalent bond formation. The bonding characteristic can be described by the ''ellipticity'' (ε) of the bonds, where the greater ε is, the more π component the bond has; the less ε is, the more σ component the bond has. Bond intensity can be measured by the electron density (ρ) of the BCP, where the greater ρ is, the more intension the bond is. The bond critical points (BCPs) and bond paths in AIM analysis are shown in Figs. 2 and 3. The cylinder-shaped cage is too long in the X-axis direction to be illustrated in the AIM view window as a whole molecule. Fig. 2 is the front view of the X-axis direction, and Fig. 3 is the side view of the X-axis direction in the three dimensions. The distances between the BCP and atom pairs, ε, ρ and $\nabla^2\rho$ of BCPs from AIM analysis of the molecule N_{78} (D_{3h}) are listed in Table 3.

Table 3
The ellipticity (ε), electron density (ρ) and the Laplacian ($\nabla^2\rho$) of the N_{78} (D_{3h}) cage at B3LYP/cc-pVDZ

	Dist. 1[a]	Dist. 2[b]	ε	ρ	$\nabla^2\rho$
35B (N_1–N_2)	0.766	0.766	0.183	0.247	−0.247
55B (N_1–N_4)	0.709	0.721	0.105	0.322	−0.616
56B (N_4–N_5)	0.739	0.746	0.106	0.285	−0.456
66B1 (N_5–N_{10})	0.740	0.745	0.199	0.282	−0.498
66B2 (N_{10}–N_{12})	0.729	0.731	0.086	0.300	−0.520
V1 ($N_4\cdots N_{12}$)	1.207	1.211	3.044	0.024	0.143
V2 ($N_{16}\cdots N_{25}$)	1.168	1.168	0.048	0.030	0.161

[a] The distance between the BCP and the first atom.
[b] The distance between the BCP and the second atom.

3. Results and discussion

The geometrical optimizations were successfully completed (see Fig. 1) at the B3LYP/cc-pVDZ level. All of the vibrational frequencies of the molecule are positive. The lowest vibrational frequency is 16 cm^{-1}. That is, the molecule structure of N_{78} (D_{3h}) is a local minimum at the B3LYP/cc-pVDZ potential energy surface. The results from NBO analysis show that the molecule has 117 σ_{N-N} covalent bonds. That is, the molecules are cage molecules with only single bonds. The results from AIM analysis (see Table 3) show that the $\nabla^2\rho$ of the BCP, of which the distances between the BCPs and atoms are less than 0.8 Å (0.8 Å is the threshold value specified by us because the length of the covalent bond should be less than $2 \times 0.8 = 1.6$ Å at B3LYP/cc-pVDZ), are less than 0.0. It indicates that the bonds in the molecule are covalent bond. The number of BCPs which $\nabla^2\rho < 0$ satisfies with the formula $3 \times 78/2 = 117$, indicates that each nitrogen atom has three covalent bonds. Meanwhile, the ε value obtained from AIM analysis shows that these bonds have the σ_{N-N} bonding characteristics. The results from AIM analysis also show that the molecule has 33 intra-molecular interactions at B3LYP/cc-pVDZ and 27 intra-molecular interactions at MP2/cc-pVDZ because $\nabla^2\rho > 0$ for the BCPs. It is noted that the B3LYP functional does not address intermolecular van der waals' interactions well because of its missing long-range correction (LC) for generalized gradient approximation (GGA) exchange [29,30] functionals. So, the single point energy calculation of the molecule at

MP2/cc-pVDZ has been carried out to verify the existence of intra-molecular interactions. The results show that there are 27 intra-molecular interactions in the molecule at MP2/cc-pVDZ. Three intra-molecular interactions between layers 2 and 5 and three intra-molecular interactions between layers 22 and 25, which can be observed at B3LYP/cc-pVDZ, are not found at MP2/cc-pVDZ. The remaining 27 intra-molecular interactions at MP2/cc-pVDZ are the same as they are at B3LYP/cc-pVDZ. Furthermore, these intra-molecular interactions are relatively "strong" because the interaction distances are short (about 2.3 Å at B3LYP/cc-pVDZ and MP2/cc-pVDZ). In this case, the intra-molecular interactions can be treated with B3LYP as with MP2.

N_1–N_2 is a typical **35B** bond. The bond length is the longest (1.529 Å, see Table 2) and the orbital energy (OE) from NBO analysis is the highest (−0.70758 a.u., see Table 2) in the molecule. Meanwhile, the electron occupancy of the orbital is lowest (1.954, see Table 2). N_1–N_2 tends to be somewhat a π bond from point of view of its ε value (0.183, see Table 3). The $\bigtriangledown^2\rho$ is −0.247, which indicates that the bond is a covalent bond. N_1–N_2 is a stronger covalent bond because the BCP has higher electron density (ρ of the BCP is 0.247.). The fact that the bond length is the longest and the OE is the highest in the molecule may be caused by steric repulsions. It can be confirmed by the total steric exchange energy (referred to as TSEE, 31.8 kcal/mol, see Table 2) from NBO analysis. The existence of steric repulsions can weaken the bond and it transfers to lower the relative stability of the molecule. On the other hand, because the bond is tend to be somewhat π bond, the bond intensity is increased and it transfers to increase the stability of the molecule. The TSEE of lone pair of N_1 is −20.4 kcal/mol (**LP1** in Table 2), and it is the lowest in the molecule. This means that the repulsion of lone pair of atom N_1 is the least. The lone pair of atom N_1 contributes to the intensity of the bonds between atom N_1 and the other atoms. The interactions of lone pairs of atoms N_1 and N_2 make N_1–N_2 tend to be a double bond. At the same time, the N_1–N_2 bond is a shared edge between a triangle and a pentagon. The fact that the triangles are the stabilizing factor [15,21] of nitrogen cages may be caused by the π bond properties of this type of bond.

N_1–N_4 is a typical **55B** bond. The bond length is the shortest (1.428 Å) and the orbital energy (OE) from NBO analysis is the lowest (−0.89766 a.u.) in the molecule. Meanwhile, the electron occupancy of the orbital is 1.975, which indicate that the number of non-localized electrons is small (2.0 − 1.975 = 0.025). N_1–N_4 is a covalent bond because its $\bigtriangledown^2\rho$ is −0.616 which is less than 0.0. The ρ value of the BCP is 0.322; it is the greatest among all of the electron densities (column ρ in Table 3), which indicates that the BCP has the highest electron density and the covalent bond is strongest in the molecule. The TSEEs of N_1–N_4 bond (−1.1 kcal/mol) and the lone pairs of atoms N_1 (−20.4 kcal/mol) and N_4 (0.4 kcal/mol) are low; these may contribute to shorten the bond length and lower the OE. Meanwhile, the electron occupancy of the lone pair of N_4 is the lowest (1.894) among all of the electron occupancies (column Occup. in Table 2). As defined above, the number of non-localized electrons is the greatest (2.0 − 1.894 = 0.106).

The non-localized electrons make the bonds between atom N_4 and the other atoms strengthen. At the same time, the N_1–N_4 bond is a shared edge between two vicinal pentagons. The fact that the pentagon is the dominant stabilizing factor [15,21] of nitrogen cages may be caused by the non-localized electrons of the lone pairs of atoms in the rings.

The properties of **56B** and **66B1** bonds are similar. The **56B** bonds only exist in the ends of the cylinder (between layers 2 and 3 and layers 24 and 25). The **66B1** bonds formed by linking the atoms in odd layers with the atoms in even layers, such as the N_5–N_{10} bond, where atom N_5 is in layer 3 and atom N_{10} is in layer 4, while **66B2** bonds formed by linking the atoms in even layers with the atoms in odd layers, such as N_{10}–N_{12} bond, where atom N_{10} is in layer 4 and atom N_{12} is in layer 5. The former bonds are parallel to the C_3 principal axis approximately, while the later are not. It brings about some differences between the two kinds of bond. The bond length of the N_5–N_{10} is 1.483 Å. It is longer than that of the N_{10}–N_{12} (1.459 Å). The OE of the N_5–N_{10} is −0.86773 a.u. It is higher than that of the N_{10}–N_{12} (−0.88356 a.u.). On the other hand, the TSEE of the N_5–N_{10} bond (−6.3 kcal/mol) is lower than that of the N_{10}–N_{12} (−0.9 kcal/mol), which means that the repulsion action of the N_5–N_{10} bond with the other orbitals is lower than that of the N_{10}–N_{12} bond. The non-localized electrons of the N_5–N_{10} bond (2.0 − 1.970 = 0.030) is greater than that of the N_{10}–N_{12} (0.016), which means that the N_5–N_{10} bond has a higher delocalization than that of the N_{10}–N_{12} bond. The delocalization contributes to the stability of the cage molecule. AIM analysis shows that there are 33 intra-molecular interactions at B3LYP/cc-pVDZ and 27 intra-molecular interactions at MP2/cc-pVDZ (see Table 1 and Fig. 2) in the molecule. The intra-molecular interactions only exist in the regions where the two atoms belong to different layers, the layer interval is 3 and the intra-molecular interactions are approximately parallel to the C_3 principal axis. Take for example, the intra-molecular interaction $N_{16}\cdots N_{25}$, where the atom N_{16} is in layer 6 (see Figs. 1 and 3) and atom N_{25} is in layer 9. The difference of the two layers is 3, and $N_{16}\cdots N_{25}$ is approximately parallel to the C_3 principal axis. In the direction of the C_3 principal axis, the intra-molecular interactions conjoin with **66B1** covalent bond in an alternating manner (e.g. $N_4\cdots N_{12}$–$N_{16}\cdots N_{25}$–$N_{28}\cdots N_{37}$, where $N_4\cdots N_{12}$ does not exist at MP2/cc-pVDZ) and form a quasi beeline. There are six such beelines in the molecule. All the beelines are approximately parallel to the C_3 principal axis (see Fig. 3). The intra-molecular interaction $N_4\cdots N_{12}$ (denoted by **V1** in Fig. 3) is near the ends of the cylinder, while the intra-molecular interaction $N_{16}\cdots N_{25}$ (denoted by **V2** in Fig. 3) lies in the midsection of the cylinder. AIM analysis shows that the distance between the two atoms N_4 and N_{12} and the BCP is about 2.28 bohr, that is, the bond path of the $N_4\cdots N_{12}$ is about 4.56 bohr at B3LYP/cc-pVDZ and at MP2/cc-pVDZ, which is transferred to the distance between the two atoms is about 2.42 Å (see Table 3), the distance between the two atoms N_{16} and N_{25} and the BCP is about 2.21 bohr both at B3LYP/cc-pVDZ and at MP2/cc-pVDZ, that is, the bond path of $N_{16}\cdots N_{25}$ is about 4.42 bohr which is transferred to the distance between the two atoms is about 2.34 Å (see Table 3) at B3LYP/cc-pVDZ

and at MP2/cc-pVDZ. The ρ of the interaction $N_4 \cdots N_{12}$ is 0.024 at B3LYP/cc-pVDZ, and it is lower than that of the interaction $N_{16} \cdots N_{25}$ ($\rho = 0.030$) at the same level. Both the difference of distances and the difference of the ρ between $N_4 \cdots N_{12}$ and $N_{16} \cdots N_{25}$ indicate that the interaction of the former is weaker than that of the latter. Especially, the ε of the interaction $N_4 \cdots N_{12}$ (3.109) is much greater than that of $N_{16} \cdots N_{25}$ (0.048) at B3LYP/cc-pVDZ, which means that the electrons scatter out of the region of the beeline between atom N_4 and atom N_{12}, while gather together in the region of the beeline between atom N_{16} and atom N_{25}. This can be verified by the results of AIM analysis at MP2/cc-pVDZ. In such a case, the BCP between the atoms N_4 and N_{12} vanishes, at the same time, the intensity of the intra-molecular interaction between atoms N_{16} and N_{25} should be invariable at B3LYP/cc-pVDZ and MP2/cc-pVDZ because the interaction distance (2.35 Å at MP2/cc-pVDZ versus 2.34 Å at B3LYP/cc-pVDZ) and the electron density (0.029, which is not listed, at MP2/cc-pVDZ versus 0.030 at B3LYP/cc-pVDZ) are almost equal to each other. This indicates that B3LYP should be used to addressing the intra-molecular interactions as MP2. Every four layers have three such interactions from layers 2 to 25 at B3LYP/cc-pVDZ and from layers 4 to 23 at MP2/cc-pVDZ. Such interactions strengthen the bonds of **56B** and **66B** and consequently make the cage molecule stable. The intra-molecular interactions contribute to the relative stabilities of the cylinder-shaped molecule. This renders the molecule to be much more stable than if it does not occur.

The enthalpy change is -4266.108637 a.u., the total energy is -4266.151406 a.u. The DFT ΔH_f [24] is 3404.2 kcal/mol. By means of the method of Ref. [24], the DFT group ΔH_f is about 43.6 kcal/mol, where the DFT group ΔH_f is the DFT ΔH_f divided by the atom number 78. It is much close to the 43.4 kcal/mol which is our prediction value in Ref. [24].

Our study show that N_{78} (D_{3h}) is a beeline molecule. The length of the cylinder-shaped molecule is about 2.5 nanometers. This molecule might be one novel nanomaterial which is environment-friendly and as a beeline nanotube or a beeline "nano-bar", it is expected to impact a wide range of applications.

4. Conclusion

The results of the study show that the nitrogen cage N_{78} (D_{3h}) is stable thermodynamically. The pentagons are the primary structural features that contribute to the stability of the molecules. Triangles in the molecular structure have a secondary stabilizing effect on the N_{78} (D_{3h}) cages. The cylinder-shaped structure of the all-nitrogen cage N_{78} (D_{3h}) is one of the stabilizing factors. These trends agree with the results of Strout and co-workers [17,23] All of the stabilizing factors are caused by the non-localization of lone pairs in the triangles and by the intra-molecular interactions of nitrogen atoms in the different layers, where the intra-molecular interactions are the dominant stabilizing feature of the molecule.

References

[1] M.N. Glukhovtsev, H. Jiao, P.V.R. Schleyer, Inorg. Chem. 35 (1996) 7124.
[2] B.M. Gimarc, M. Zhao, Inorg. Chem. 35 (1996) 3289.
[3] M. Tobita, R.J. Bartlett, J. Phys. Chem. A 105 (2001) 4107.
[4] L.J. Wang, P. Warburton, P.G. Mezey, J. Phys. Chem. A 106 (2002) 2748.
[5] Q.S. Li, D. Yong, J. Phys. Chem. A 106 (2002) 9538.
[6] L.J. Wang, W.G. Xu, Q.S. Li, J. Mol. Struct. (THEOCHEM) 531 (2000) 135.
[7] A.M. Tian, F.J. Ding, L.F. Zhang, Y.M. Xie, H.F. Schaefer III, J. Phys. Chem. A 101 (1997) 1946.
[8] T.M. Klapötke, R.D. Harcourt, J. Mol. Struct. (THEOCHEM) 541 (2001) 237.
[9] R. Engelke, J.R. Stine, J. Phys. Chem. A 94 (1990) 5689.
[10] C. Chen, S.F. Shyu, Int. J. Quant. Chem. 73 (1999) 349.
[11] D.L. Strout, J. Phys. Chem. A 106 (2002) 816.
[12] M.R. Manaa, Chem. Phys. Lett. 331 (2000) 262.
[13] Y. Ren, X. Wang, N.B. Wong, A.M. Tian, F.J. Ding, L.F. Zhang, Int. J. Quant. Chem. 82 (2001) 34.
[14] F.J. Owens, J. Mol. Struct. (THEOCHEM) 623 (2003) 197.
[15] L.J. Wang, P. Warburton, M.Z. Zgierski, Chem. Phys. Lett. 391 (2004) 338.
[16] H.W. Zhou, W.X. Zheng, X. Wang, Y. Ren, N.B. Wong, Y.J. Su, A.M. Tian, J. Mol. Struct. (THEOCHEM) 732 (2005) 139.
[17] L.Y. Bruney, T.M. Bledson, D.L. Strout, Inorg. Chem. 42 (2003) 8117.
[18] Q.S. Li, J.F. Zhao, J. Phys. Chem. A 106 (2002) 5367.
[19] J. Guan, L.P. Cheng, W.G. Xu, Q.S. Li, S. Li, Z.P. Zhang, J. Theor. Comput. Chem. 2 (2003) 7.
[20] J. Guan, S.W. Zhang, W.G. Xu, Q.S. Li, Struct. Chem. 15 (2004) 121.
[21] J.D. Gu, K.X. Chen, H.L. Jiang, J.Z. Chen, R.Y. Ji, Y. Ren, A.M. Tian, J. Mol. Struct. (THEOCHEM) 428 (1998) 183.
[22] T.K. Ha, O. Suleimenov, M. Nguyen, Chem. Phys. Lett. 315 (1999) 327.
[23] D.L. Strout, J. Phys. Chem. A 108 (2004) 2555.
[24] H.W. Zhou, N.B. Wong, G. Zhou, A.M. Tian, J. Phys. Chem. A 110 (2006) 3845.
[25] L.J. Wang, P.G. Mezey, J. Phys. Chem. A 109 (2005) 3241.
[26] M.J. Frisch, G.W. Trucks, H.B. Schlegel, G.E. Scuseria, M.A. Robb, J.R. Cheeseman, V.G. Zakrzewski, J.A. Montgomery Jr., R.E. Stratmann, J.C. Burant, S. Dapprich, J.M. Millam, A.D. Daniels, K.N. Kudin, M.C. Strain, O. Farkas, J. Tomasi, V. Barone, M. Cossi, R. Cammi, B. Mennucci, C. Pomelli, C. Adamo, S. Clifford, J. Ochterski, G.A. Petersson, P.Y. Ayala, Q. Cui, K. Morokuma, D.K. Malick, A.D. Rabuck, K. Raghavachari, J.B. Foresman, J. Cioslowski, J.V. Ortiz, A.G. Baboul, B.B. Stefanov, G. Liu, A. Liashenko, P. Piskorz, I. Komaromi, R. Gomperts, R.L. Martin, D.J. Fox, T. Keith, M.A. Al-Laham, C.Y. Peng, A. Nanayakkara, C. Gonzalez, M. Challacombe, P.M.W. Gill, B.G. Johnson, W. Chen, M.W. Wong, J.L. Andres, M. Head-Gordon, E.S. Replogle, J.A. Pople, Gaussian 98, Revision A.11, Gaussian Inc., Pittsburgh, PA, 1998.
[27] F. Weinhold, NBO 5.0 Program Manual, Theoretical Chemistry Institute and Department of Chemistry, University of Wisconsin, Madison, Wisconsin 53706, pp. 101–103.
[28] R.F.W. Bader, Atoms in Molecules, A Quantum Theory; International Series of Monographs in Chemistry, 22, Oxford University Press, Oxford, 1990.
[29] T.A. Sato, T.B. Tsuneda, K. Hirao, J. Chem. Phys. 123 (2005) 1.
[30] J.M. Molina, J.A. Dobado, M.C. Daza, J.L. Villaveces, J. Mol. Struct. (THEOCHEM) 580 (2002) 117.